受入
79-8-120
高工研図書室

EUROPEAN ORGANIZATION FOR NUCLEAR RESEARCH

CERN EP/79-49
21 May 1979

SEMICOHERENT ELASTIC PION-CARBON SCATTERING AT 25 AND 40 GeV/c

P.L. Frabetti

Istituto di Fisica dell'Università and INFN, Bologna, Italy

G. Bellini, T. Bettinazzi, M. Di Corato, E. Meroni, S. Micheletti, F. Palombo, F. Ragusa, P.G. Rancoita*) and G. Vegni

Istituto di Fisica dell'Università and INFN, Milano, Italy

L. Chernenko, Yu. Ivanshin, I. Pisarev, S. Sychkov, A. Tjapkin, V. Vishniakov and O. Zaimidoroga

Joint Institute for Nuclear Research, Dubna, USSR

P.F. Manfredi**)

Polytechnic School and Sezione, INFN, Milano, Italy

(Submitted to Nuclear Physics)

*) Present address: CERN, Geneva, Switzerland.

**) Present address: Facoltà di Ingegneria, Università di Pavia, Italy.

ABSTRACT

In the frame of a systematic study of hadron-nucleus interactions performed at the Serpukhov accelerator (CERN-IHEP 5th experiment), semicoherent elastic scattering on carbon $\pi^- - {}^{12}C \rightarrow \pi^- - {}^{12}C^*$ (4.44 MeV) was investigated with 25 and 40 GeV/c incident pions.

The experimental data were obtained with a counter technique, looking at the coincidence between the scattered pion and the 4.44 MeV photon from the $J^P = 2^+$ carbon excited state detected by a NaI counter.

The value obtained for the integrated cross-section at 40 GeV/c in the $0.0032 \leq t \leq 0.27$ $(GeV/c)^2$ four-momentum transfer range is

$$\sigma = 1.19 \pm 0.12 \text{ mb} .$$

According to the theoretical models, this t-range at 40 GeV/c covers more than 99% of the angular distribution, so the above value almost corresponds to the total semicoherent elastic cross-section.

At 25 GeV/c the t-range was $0.0013 \leq t \leq 0.10$ $(GeV/c)^2$; the corresponding integrated cross-section is

$$\sigma = (0.80 \pm 0.25) \text{ mb} .$$

In this case the correction to be applied to obtain the total cross-section is model-dependent.

A possible contamination from the decay of A = 11 excited states has been investigated; because of this contamination, a reduction of 10% of the above cross-sections cannot be excluded.

1. INTRODUCTION

In the last few years many experiments have been devoted to high-energy hadron-nuclei interactions in order to use the filtering properties of the nuclei in selecting specific hadron state production, and with the purpose of arriving at a better understanding of how hadron systems propagate and are absorbed in nuclear matter.

These experiments are mainly concerned with the coherent channels, in which the target nuclei remain in the ground state throughout the whole process, or with the multiparticle production channels, in which no particular states are selected *a priori* but the nucleus is, in most cases, fragmented.

Somehow between these extreme cases there are the so-called "semicoherent reactions" where, after being struck by the incoming projectile, the nucleus is left in a well-determined excited state.

Semicoherent high-energy interactions can be used to select the production of specific hadronic systems, as first suggested by Piccioni [1] and Stodolsky [2]. Carbon is a particularly suitable target nucleus because of its $J^P = 2^+$, $I = 0$, 4.44 MeV first excited level. This level is reached in interactions in which no quantum number but only pure angular momentum is exchanged: the most typical cases are the diffraction-like interactions, e.g.

$$\begin{aligned} h + {}^{12}C &\rightarrow h^* + {}^{12}C^*(2^+) \\ &\hookrightarrow {}^{12}C + \gamma\ (4.44\ \text{MeV}) \ . \end{aligned} \qquad (1)$$

Experiments have already been performed with incident protons and incident pions at intermediate values of momentum (0.68-6 GeV/c) [1,3-5]. In these experiments attention was mainly paid to the simplest of type (1) reactions, namely the semicoherent elastic scattering. The data were compared with theoretical calculations performed on the basis of the DWIA or Glauber models by using electron-carbon scattering data for the 2^+ (4.44 MeV) transition nuclear densities. In all cases the calculated π-C semicoherent elastic scattering cross-sections were found to be about a factor of 2 higher than the experimental ones.

In order to investigate the semicoherent interactions at high energy we started, as in the case of the quoted experiments at lower energies, with the elastic scattering, because the best approach to these phenomena is first to understand the simplest of the channels.

In this paper, we shall describe the apparatus used and give the results of the measurement of the total cross-section for the reaction

$$\pi^- + {}^{12}C \rightarrow \pi^- + {}^{12}C^*(2^+) \hookrightarrow {}^{12}C + \gamma\ (4.44\ \text{MeV}) \qquad (2)$$

performed in Serpukhov, using the facilities of the high-statistics experiment on coherent production [6]. To the coherent set-up we have added a "vertex detector" to detect the 4.4 MeV γ's and to reject, by anticoincidence, incoherent nuclear events. Most of events were collected with 40 GeV/c incident pions; also, a sample of data at 25 GeV/c was taken.

Preliminary results at 40 GeV/c have been already published [7]. The analysis of the angular distributions for the semicoherent scattered pions is still going on.

With the analysis of present data in progress, Bertocchi and Troncon have published [8] a new theoretical calculation for reaction (2). This calculation was performed in the framework of the Glauber theory, using the formalism of harmonic solid tensors and the inelastic form factor for the nuclear transition extracted from the inelastic electron-carbon scattering. The theoretical results are in good agreement with the low-energy experimental data for both proton- and pion-induced reactions.

The present paper consists of the following parts: Section 2 describes the experimental set-up, and Section 3 is devoted to the data collection. The data analysis, the efficiency calculations, and the effect of γ contaminations from the decay of mass-11 nuclei are discussed in Sections 4, 5, and 6, respectively. Final results on cross-section values and the conclusions are reported in Section 7.

2. EXPERIMENTAL SET-UP

The data presented here were collected using, in part, the set-up of the Dubna-Milan high-statistics experiment on coherent production at 40 GeV/c induced by π^- and K^- beams [6].

The complete description of the set-up will be published elsewhere. Here attention is focused on the parts of the set-up used for the semicoherent data collection.

2.1 Spectrometer for charged forward particles

Figure 1 shows a sketch of the set-up: Scintillation counters S_1 S_3 S_4 S_n in coincidence and $\bar{A}_3$ in anticoincidence were used to define the beam; Čerenkov counters $\check{C}_2$ $\check{C}_3$ were used to select π^- in the incident negative beam.

The target (LT, live target) consisted of a 5×5 cm^2 section, 10 cm long polystyrene plastic scintillator counter (50% C, 50% H) viewed by a 56 AVP photomultiplier. Veto counters surrounded the LT laterally, except for the side terminating at the light-guide. The use of the LT signal to reduce the incoherent background will be discussed below. A scintillator-lead sandwich G_{2-6} was used to veto forward-emitted charged and neutral particles in the angular range $\theta \geq 12.9 \pm 0.8$ mrad in the lab. system (a sample of the 25 GeV/c data was collected using only G_{4-6} in the trigger; in this case the angular range was 19 mrad).

A multiwire proportional chamber (MWPC) [9] was located inside the 5 m long magnet of the MIS spectrometer, the central field of which was kept at 17.58 ± 0.01 kG. This chamber consists of two orthogonal planes; its active area is 60×60 cm^2. The related electronics includes 600 signal conditioning channels (as many as the wires), a fast majority processor, and a read-out system interfaced to an HP 2100 A computer to check the chamber efficiency. The MWPC fast majority logic supplies a signal proportional to the numbers of particles passing through it.

Usually the signal $[(x \geq 2) \cdot \mathrm{OR} \cdot (y \geq 2]$ *) from the MWPC, gated by the fast signal S_3 S_n $\bar{A}_3$ $\bar{K}$, was employed in anticoincidence to reject many-prong events.

---

*) x and y are the majority coincidence signals for the two planes.

The $[(x \geq 2) \cdot \text{AND} \cdot (y \geq 2)]$ logic was also used. The trigger efficiency in this case was found to be the same as if the events with two particles in only one plane were rejected off line.

A scintillation counter K, located 7 m after the magnet, vetoed the non-interacting beam particle. The counter K defines a lower acceptance angle of 1.4 ± 0.3 mrad.

The triggers, including the NaI γ detector, which will be described below, were

$$T_1 = S_1\ S_3\ S_4\ \bar{C}_2\ \bar{C}_3\ S_n\ \bar{A}_3\ \bar{K}\ \text{LT}\ \bar{V}\ \bar{G}_{2-6}\ \overline{\text{MW}(x \geq 2 \cdot \text{OR} \cdot y \geq 2)}\ \text{NaI}$$

and

$$T_2 = S_1\ S_3\ S_4\ \bar{C}_2\ \bar{C}_3\ S_n\ \bar{A}_3\ \bar{K}\ \text{LT}\ \bar{V}\ \bar{G}_{4-6}\ \overline{\text{MW}(x \geq 2 \cdot \text{OR} \cdot y \geq 2)}\ \text{NaI}\ .$$

2.2 Detection of the 4.44 MeV γ-rays

The 4.44 MeV γ-rays coming from the $^{12}C^*$ decay were detected by a NaI (Tl) crystal, 5 inches in diameter, 5 inches long, viewed by a 58 AVP photomultiplier.

The axis of the NaI intersected the live target (LT) in the horizontal plane (Fig. 1b).

The distance from the centre of the LT to the nearest edge of the crystal was 8.5 cm.

The last dynode of the PM was kept at zero voltage, and a positive voltage source with a large current capability was connected to the anode in order to avoid both saturation and count rate effects, and also to have enough sensitivity on the anode signal to permit calibration with a standard ^{60}Co γ-ray source (1.17, 1.33 MeV).

Timing information was taken from the anode, using a constant fraction discriminator with the threshold set just above the noise level. The linear signal instead was extracted from the last dynode, processed by a linear chain, and then sorted by a LeCroy 2249A analog-to-digital converter (ADC). Very low intensity (40,000 particles per 1.5 s spill) was used to avoid counting-rate effects.

3. DATA COLLECTION

The number of incident π's, the number of interactions, and the veto counter random coincidences were checked on line and recorded, together with all the pulse heights needed, through fast scalers and ADCs using a CAMAC system interfaced to an HP 2100A computer. On-line statistics and spectra for about 90% of the events were provided, allowing a real-time monitoring and a rough analysis.

About 35,000 triggers were collected at 40 GeV/c and 10,000 at 25 GeV/c.

Every 2-3 hours of running time a calibration of the NaI counter with a ^{60}Co γ source was repeated.

Figure 2 shows a typical calibration pulse-height distribution for the NaI counter. The signals of the two γ's (1.17 MeV and 1.33 MeV) are evident, with an energy resolution estimated at around 10% FWHM at 1.33 MeV.

4. DATA ANALYSIS

4.1 40 GeV/c data

The data analysis was performed on 35,000 semicoherent T_1 triggers corresponding to 1.13×10^8 40 GeV/c incident π's. At this momentum the angular acceptance (1.4 ± 0.3)-(12.9 ± 0.8) mrad corresponds to the (0.0032 ± 0.0013)-(0.27 ± 0.03) $(GeV/c)^2$ t-range. The data were first analysed in separate samples of about 10,000 triggers. In order to reduce the effect of the long-term instability of the NaI counter, each sample of the NaI pulse-height distribution was fitted (see below). Subsequently the samples were added, in accordance with the base-line positions obtained in the fits. The gain in stability was found to be of the order of a few percent, while the base-line level was constant within the required accuracy.

Figure 3 shows the pulse-height distribution of the NaI counter for the total statistics at 40 GeV/c. The solid line is our fit, which will be discussed later.

4.2 25 GeV/c data

Although the experiment was mainly devoted to 40 GeV/c data, a sample of 10,000 events at 25 GeV/c with the T_1 trigger, corresponding to 2.33×10^7 incident π's, and a sample of 4000 events using the T_2 trigger were also collected. The

t-range was $(0.0013 \pm 0.0006)-(0.10 \pm 0.02)$ $(GeV/c)^2$ with trigger T_1, and $0.0013-0.23$ $(GeV/c)^2$ with T_2.

Figure 4 shows the NaI pulse-height distribution for the T_1 triggers. The T_2 triggers were used only in order to test the correction for the angular upper limit cut.

4.3 The LT selection

To reduce background in the NaI spectrum, the events were selected according to the energy released in the polystyrene target.

Figure 5 shows the LT pulse-height distribution corresponding to beam particle triggers.

Semicoherent events should give rise to the same distribution because the effect produced by nuclei recoils is negligible (the energy of the recoiling $^{12}C^*$ is of the order of a few MeV, but the corresponding light output is greatly reduced by quenching effects) [10].

Figure 6 shows the LT spectrum for semicoherent triggers. The high-energy tail is due to incoherent events with a large energy release in the target.

The NaI pulse-height distribution at 40 GeV/c, selected with the criterion of an upper energy threshold on the LT signal (ADC channel ≤ 260), is shown in Fig. 7. Note that the signal-to-background ratio is improved by a factor of about 2.

4.4 NaI pulse-height analysis

The NaI pulse-height distribution was analysed by means of a Monte Carlo fit. The NaI response to 4.44 γ's was first calculated with a Monte Carlo program (GAMMA) [11]. This program took into account the different interactions of a γ within our 5 inch long, 5 inch diameter NaI detector and calculated the energy released in the detector.

The energy distribution thus obtained was folded with a Gaussian featuring an energy-dependent width, then weighted with a free parameter and added to a polynomial background. The resulting χ^2 function was minimized. This procedure was applied to the 40 GeV/c and the 25 GeV/c NaI spectra with and without the LT selection. The results of the fits are shown in Table 1.

In the 40 GeV/c distribution, we tried to take into account also the broad enhancement at 2 MeV due to the reactions

$$\pi^- + {}^{12}C \rightarrow \pi^- + \begin{cases} n + {}^{11}C^*(\tfrac{1}{2}^-) \\ \qquad \hookrightarrow {}^{11}C + \gamma\ (2\ \text{MeV}) & (3a) \\ p + {}^{11}B^*(\tfrac{1}{2}^-) \\ \qquad \hookrightarrow {}^{11}B + \gamma\ (2\ \text{MeV})\ . & (3b) \end{cases}$$

To do this, the NaI response to a 2 MeV γ was calculated in the same way as before, and added to the previous function to evaluate the χ^2. Results of the fit are shown in Table 1 and Figs. 3 and 7.

5. EFFICIENCY CALCULATIONS

Table 2 shows a list of corrections that were applied to the "4.44 events" in order to calculate integrated cross-sections.

The corrections, due to δ-rays, random coincidences in $\bar{K}$ and $\bar{G}$ counters, and MWPC efficiency, were found to be negligible in comparison with those considered below.

The entries of Table 2 are as follows:

a) ε_1: NaI efficiency

The NaI intrinsic efficiency was calculated with the same program GAMMA used for the energy released in the γ detector [11]. The efficiency was evaluated as the ratio of the numbers of interacting photons to the photons hitting the detector, irrespective of the amount of energy released.

b) ε_2: NaI geometrical efficiency

The vertex geometry was reproduced with a Monte Carlo program, also taking into account the effect of the quadrupole transition of the ${}^{12}C^*$ (4.44) level. In order to evaluate the NaI geometrical efficiency, the 4.44 MeV γ was emitted with a distribution proportional to $\sin^2 2\theta$, θ being the angle between recoiling nucleus and γ direction [12].

c) ε_3: LT Landau tail loss

This correction was applied to the LT ch. $\leq$ 260 sample. In fact, because of the Landau tail for relativistic particles, the LT cut rejected parts of the

semicoherent events that were expected to give the same LT pulse-height distribution as the beam particles. Therefore this correction was calculated on the basis of the experimental LT spectrum (Fig. 3), for beam particles crossing the target without interactions.

d) ε_4: double interactions in the target

Owing to the length of the target (10 cm), the probability of an inelastic pion interaction before or after a semicoherent interaction was not negligible. This effect was calculated on the basis of the inelastic $\pi^- - {}^{12}C$ and π^--p cross-sections at 40 GeV/c and 25 GeV/c.

e) γ absorption in the LT and veto counter

This correction took into account the probability of interaction of the 4.44 MeV γ's in the LT and in the veto counter positioned between the LT and the NaI detector.

6. ^{11}B and ^{11}C NUCLEI CONTAMINATION

A possible source of contamination in the γ spectrum for reaction (1) could be due to the reactions:

$$\pi^- + {}^{12}C \rightarrow \pi^- + \begin{cases} n + {}^{11}C^* \ (3/2^-) \\ \qquad \hookrightarrow {}^{11}C + \gamma \ (4.8 \text{ MeV}) & (4a) \\ p + {}^{11}B^* \ (3/2^-) \\ \qquad \hookrightarrow {}^{11}B + \gamma \ (5.0 \text{ MeV}) \ . & (4b) \end{cases}$$

Since data on the above reactions are not known at the energies of the present experiment, a mechanism was assumed (using the impulse approximation), similar to that of the low-energy pick-up reactions $^{12}C(x,x')^{11}B^*$ or $^{12}C(y,y')^{11}C^*$.

These reactions strongly excite the 2 MeV ($J^P = 1/2^-$) and the 4.8-5 MeV ($J^P = 3/2^-$) states of the residual nucleus, but there is only weak excitation of the 4.4 MeV ($J^P = 5/2^-$) state [13]. As ^{11}B and ^{11}C are mirror nuclei, they are expected to give the same contributions to these lines. The actual resolution did not allow *a priori* discrimination in the γ spectra of a possible 4.8-5 MeV contamination from the 4.44 MeV semicoherent peak. Under the above hypothesis,

we obtained from the low-energy pick-up data a ratio 2.6 to 1 for the intensities of the 2 MeV and 4.8-5 MeV lines*). Consequently, taking into account the intensity of the 2 MeV line in our spectrum, it can be expected that about 10% of the "4.44 MeV" events should be attributed to a 4.8-5 MeV $^{11}A^*$ contamination.

In a completely independent way, this contamination can be estimated from the effect produced on the "4.44 MeV" sample by applying the already described cut on the LT pulse-height distribution (LT ch. $\leq$ 260). In this way an $^{11}A^*$ contamination of 8% **) of the "4.44 MeV" events is obtained, which is quite compatible with the previous one.

It should be stressed, however, that the effect produced by the LT selection is also compatible, within the errors, with the complete absence of contamination. Consequently, if the information deduced from the low-energy pick-up reactions (on the 2 MeV/4.8-5 MeV relative intensities) could not be applied to the present reactions, it would not be possible to discriminate between $\sim$ 10% of $^{11}A^*$ contamination or zero contamination.

7. CROSS-SECTIONS AND CONCLUSIONS

As already pointed out, at 40 GeV/c the actual angular acceptance corresponds to a t-range $(0.0032 \pm 0.0013) \leq t \leq (0.27 \pm 0.03)$ $(GeV/c)^2$. More than 99% of the differential cross-section is included in this t-range in any of the proposed models [1,4,8], and it can be assumed that the integrated cross-section corresponds closely to the total elastic semicoherent cross-section.

From the number of events in the 4.44 MeV peak, coming from the fit and neglecting the LT information (see Table 1, first line, and Fig. 5), and with

---

*) In the pick-up reactions the 2 MeV and 4.8-5 MeV states are excited with relative strengths 1.8 to 1 [13]. The 2 MeV state decays directly to the ground state; the 4.8-5 MeV decays in 17% of the cases to the 2 MeV state and, for the remaining cases, directly to the ground state [13]. Taking into account also the different NaI counter intrinsic acceptances for the two energies, a 2.6 to 1 ratio is obtained for the intensities of the two gamma signals.

**) As already described, the LT cut reduces the "4.44 MeV" sample by about 15%. The cut in the "Landau tail" should produce a reduction of about 13% on the "real $^{12}C^*$" sample; on the other hand, this cut should reject about 80% of the proton recoils in reaction (4b) and it will virtually not affect the neutron recoils of reaction (4a), producing a total reduction of $\sim$ 40% on a possible 4.8-5 MeV line coming from $^{11}A^*$ decay. It is found that 223 $\pm$ 50 events corresponding to about 8% of the total "4.44 MeV" peak, could be attributed to this contamination effect.

the corrections listed in Table 2 (first line), for reaction (2) the following value of σ is obtained at 40 GeV/c:

$$\sigma = 1.19 \pm 0.12 \text{ mb} .$$

From the sample selected according to the LT pulse-height cut discussed above (see Table 1, second line, and Fig. 6) and after applying the efficiency corrections also for the Landau tail cut (second line of Table 2), for the same reaction we obtained the value

$$\sigma = 1.16 \pm 0.11 \text{ mb} ,$$

which is consistent with the previous one.

As pointed out in detail in Section 6, on the basis of the intensity of the 2 MeV line and applying the 2 MeV/4.8-5 MeV ratio obtained in low-energy reactions, a 10% contamination of the 4.44 MeV sample from the 4.8-5 MeV γ of the A = 11 excited nuclei [reactions (4a) and (4b)] is possible. Consequently the elastic cross-section would be reduced by the same amount.

At 25 GeV/c incident momentum the angular acceptance corresponds to the $(0.0013 \pm 0.0006) \leq t \leq (0.10 \pm 0.02)$ $(\text{GeV/c})^2$ range.

The correction to be applied to obtain the total elastic cross-section depends critically on the shape of the t-distribution (e.g. in a t-distribution of the type [1] $t^2 \times e^{-4.3t}$, the present interval covers 82% of the total cross-section).

Therefore the value of the integrated cross-section will be restricted to the t-interval defined above, but the error given includes the experimental incertitude on the t-limits, evaluated by taking into account the proposed models for the t-distribution.

In this case, from Tables 1 and 2, as described above, it follows that

$$\sigma = 0.80 \pm 0.25 \text{ mb} .$$

It is not possible to investigate the contamination due to A = 11 nuclei decay, because of the large statistical errors in the γ spectrum.

In the model of Bertocchi and Troncon, the total cross-section for reaction (2) at 40 GeV/c is calculated to be 1.20 mb; at 25 GeV/c these authors obtain

σ = 1.18 mb in the t-interval ($0.0013 \leq t \leq 0.10$) $(GeV/c)^2$ (see [8] and private communication).

It can be concluded that also at high energies, such as those available at the Serpukhov accelerator, the semicoherent processes are very evident and measurable. A possible contamination for A = 11 nuclei should be considered. In any case a quite good agreement, especially for the point at 40 GeV/c, is found with the calculation, developed by Bertocchi and Troncon, in the frame of the Glauber theory.

Acknowledgements

We would like to thank H.S. Plendl for very useful suggestions on the problem of the A = 11 nuclei contamination. We feel particularly indebted to L. Bertocchi and C. Troncon for the stimulating and frequent discussions on the subject. We are grateful to C. Meroni for her important contribution to the analysis of the data.

REFERENCES

[1] W. Melhop et al., Proc. Topical Seminar on High-Energy Collisions Involving Nuclei, Trieste, 1974 (Editrice Compositori, Bologna, 1975), p. 85.

[2] L. Stodolsky, Phys. Rev. 144 (1966) 1145.

[3] L.J. Koester et al., Proc. Topical Seminar on High-Energy Collisions Involving Nuclei, Trieste, 1974 (Editrice Compositori, Bologna, 1975), p. 113.

[4] J.L. Groves et al., Phys. Rev. D 15 (1977) 47.

[5] R.J. Wojslav, Ph.D. Thesis, Univ. Illinois, Urbana, Ill.

[6] Bologna-JINR-Milano Collaboration, CERN PH I/COM-73/32 (1973).

[7] T. Bettinazzi et al., π^- carbon semicoherent elastic cross-section at 40 GeV/c, Proc. Triangle Seminar on Recent Developments in High-Energy Physics, Campione d'Italia, 1977 (Editrice Compositori, Bologna, 1978), p. 429.

[8] L. Bertocchi and C. Troncon, Hadron-induced semicoherent scattering and the excitation of the $^{12}C(2^+, 4.44$ MeV) level, Trieste report IC/77/151.

[9] G. Colla et al., Nucl. Instrum. & Methods 148 (1978) 487.

[10] J.B. Birks, The theory and practice of scintillation counting (Pergamon Press, Oxford, 1964), p. 185.

[11] M. Belluscio et al., Nucl. Instrum. & Methods 118 (1974) 553.

[12] A. Clegg, High-energy nuclear reactions (Clarendon Press, Oxford, 1965), p. 58.

[13] F. Ajzenberg-Selove, Nucl. Phys. A248 (1975) 1, and references cited therein.

Table 1

Fit results

	4.44 MeV events	2 MeV events	χ^2	Degrees of freedom
40 GeV/c no LT selection	2745^{+140}_{-136}	698^{+109}_{-118}	25.2	31
40 GeV/c LT ch. ≤ 260	2324^{+116}_{-111}	325^{+75}_{-73}	24.18	31
25 GeV/c no LT selection	373^{+52}_{-44}	(a)	31	31
25 GeV/c LT ch. ≤ 260	339^{+46}_{-44}	(a)	30	25

(a) Owing to lack of statistics in the 25 GeV/c sample, we have not extended the fit to the 2 MeV region.

Table 2

Efficiency parameters

	ε_1 NaI intrinsic efficiency	ε_2 NaI geometric efficiency	ε_3 LT cut loss energy	ε_4 double interactions in target effect	ε_5 γ absorption in LT or in veto effect
No LT cut	0.503 ± 0.022	0.102 ± 0.006	1	0.90 ± 0.02	0.91 ± 0.01
LT ch. ≤ 260	0.503 ± 0.022	0.102 ± 0.006	0.868 ± 0.005	0.90 ± 0.02	0.91 ± 0.01

(The corrections are obtained by dividing the numbers of events by the ε_i values.)

Figure captions

Fig. 1 : Experimental set-up:

a) General layout;

b) Vertex detectors.

Fig. 2 : Calibration pulse-height distribution (^{60}Co γ's).

Fig. 3 : Pulse-height distribution for T_1 trigger events at 40 GeV/c. The full line represents the over-all fit, the dashed line the fitted background.

Fig. 4 : Pulse-height distribution for T_1 trigger events at 25 GeV/c. The full line represents the over-all fit, the dashed line the fitted background.

Fig. 5 : Live target (LT) pulse-height spectrum for beam particles; the dashed line indicates channel 260 (see text).

Fig. 6 : Live target (LT) pulse-height spectrum for the semicoherent T_1 trigger; the dashed line indicates the position of the cut (channel 260).

Fig. 7 : The same as fig. 3 but with LT channel $\leq$ 260 selection.

a) GENERAL LAYOUT

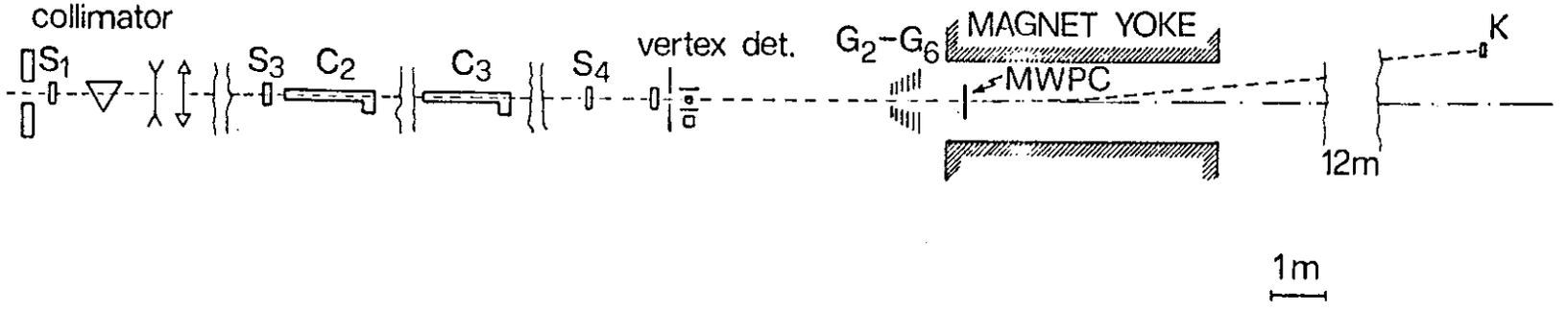

b) VERTEX DETECTOR

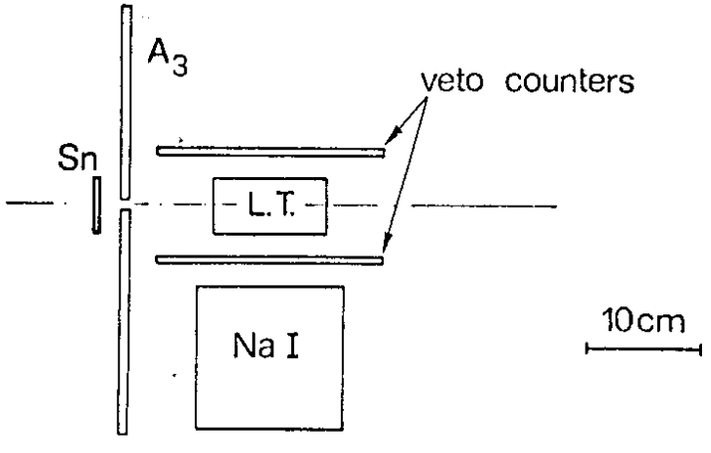

Fig. 1

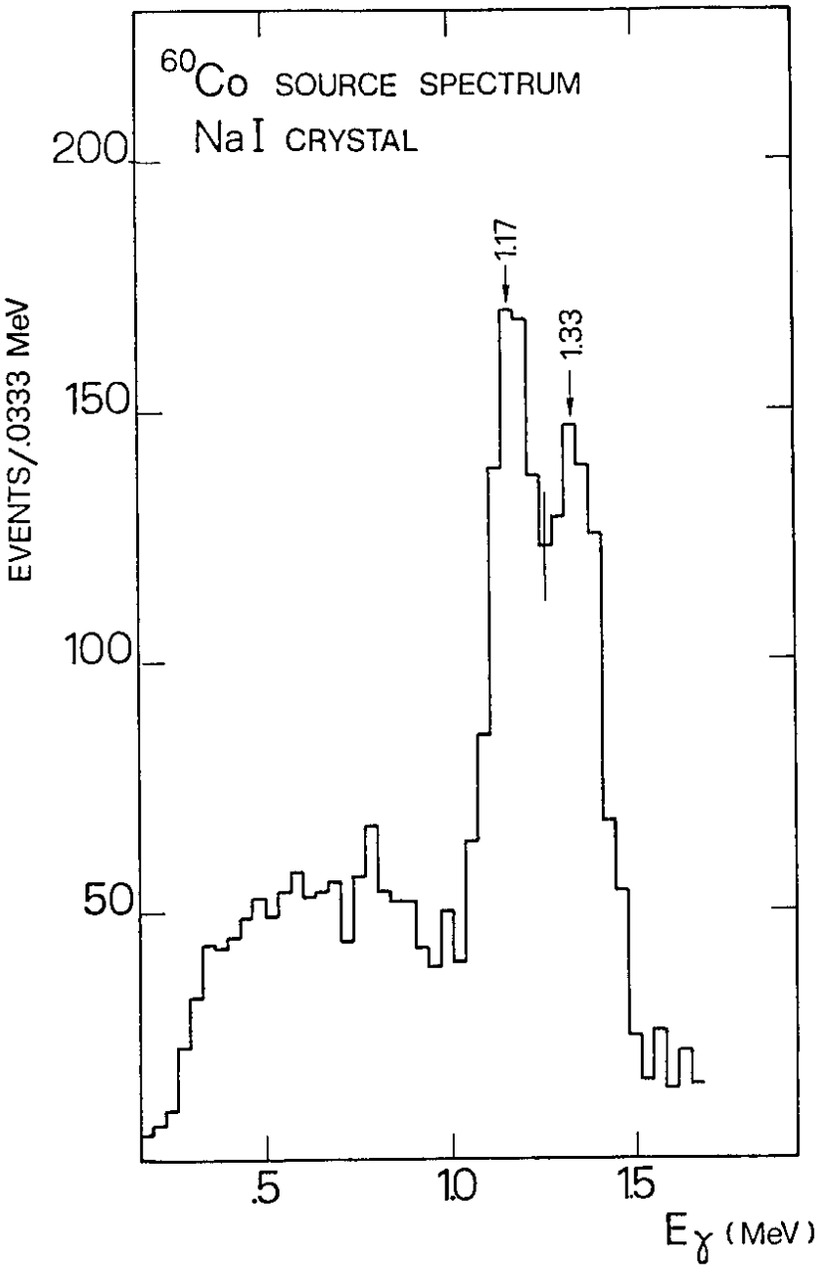
^{60}Co SOURCE SPECTRUM
NaI CRYSTAL
200
150
100
50
EVENTS/.0333 MeV
1.17
1.33
.5
1.0
1.5
E_γ (MeV)

Fig. 2

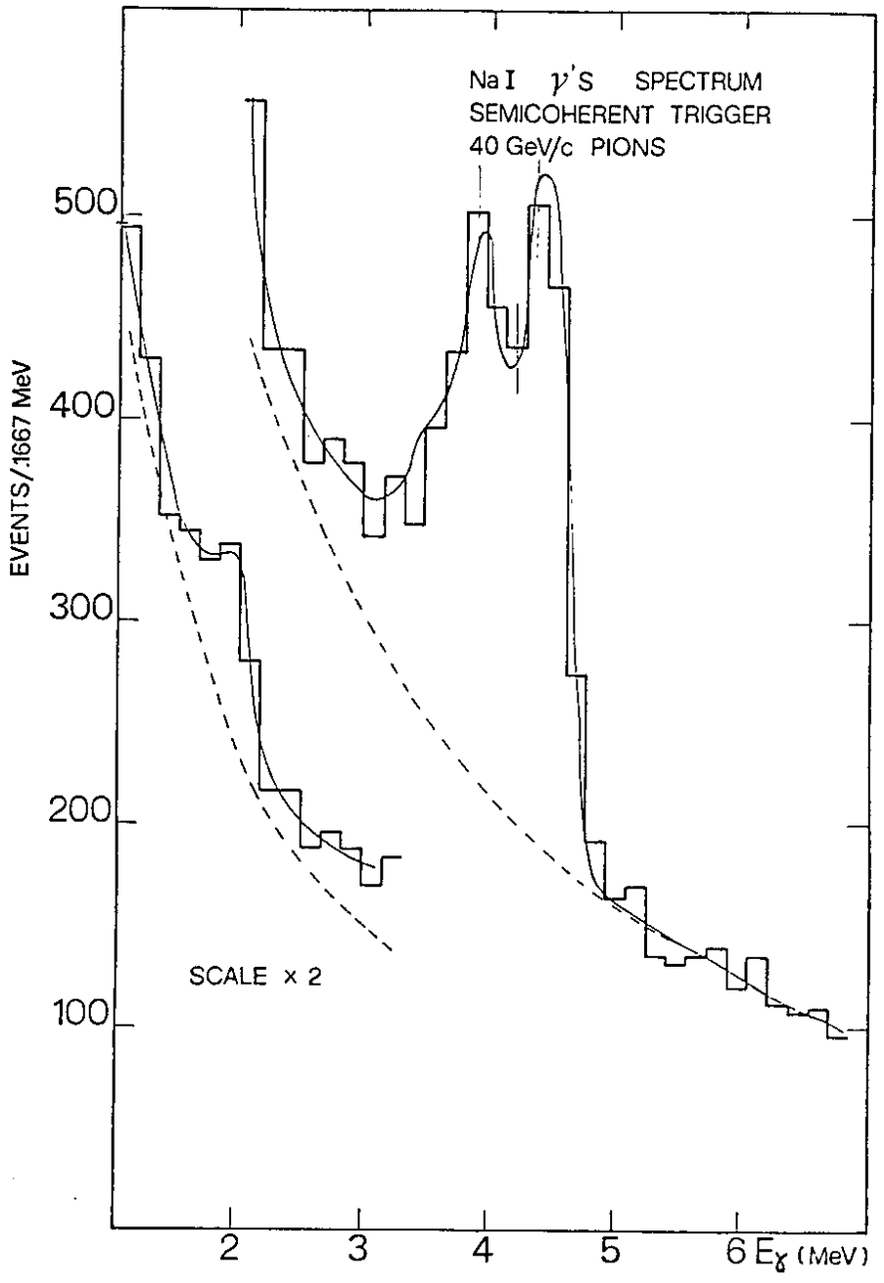
NaI γ'S SPECTRUM
SEMICOHERENT TRIGGER
40 GeV/c PIONS
EVENTS/.1667 MeV
500
400
300
200
100
SCALE x 2
2
3
4
5
6 Eγ (MeV)

Fig. 3

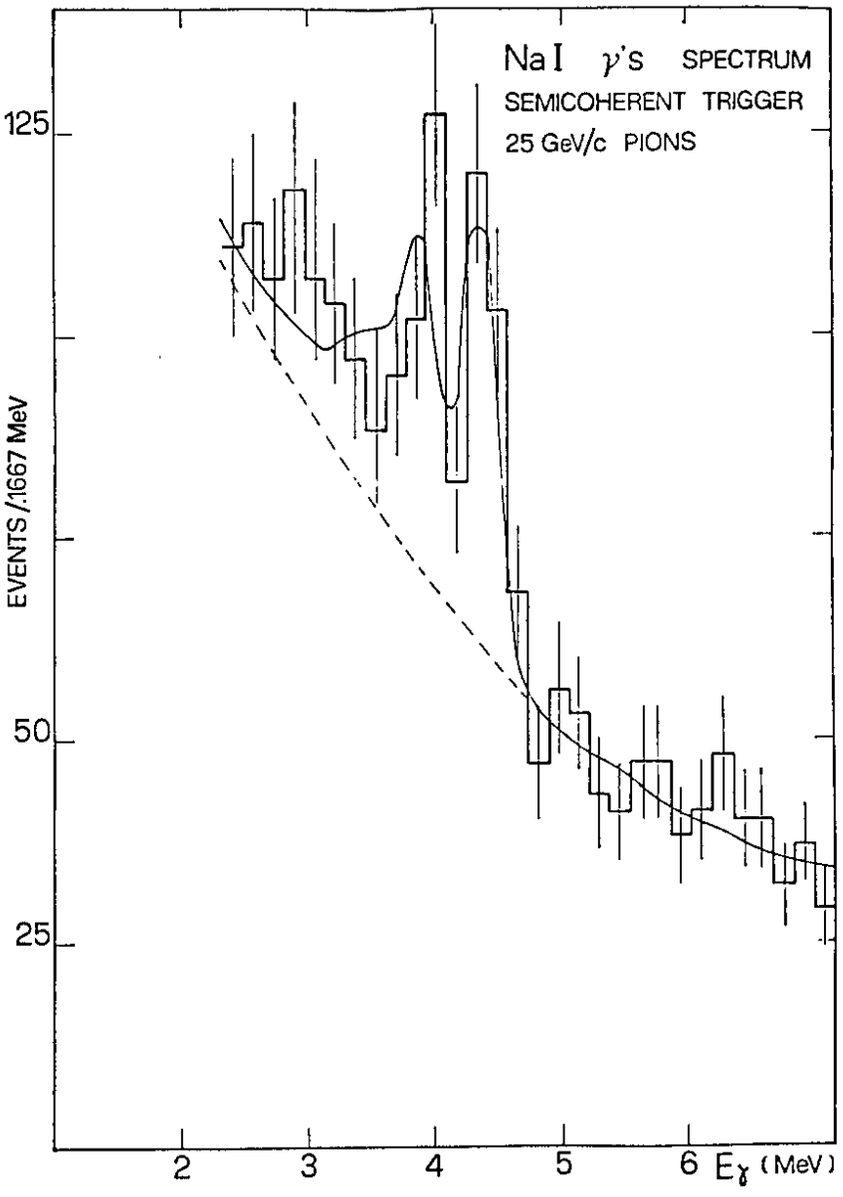
NaI γ's SPECTRUM
SEMICOHERENT TRIGGER
25 GeV/c PIONS
EVENTS /1667 MeV
125
50
25
2
3
4
5
6
Eγ (MeV)

Fig. 4

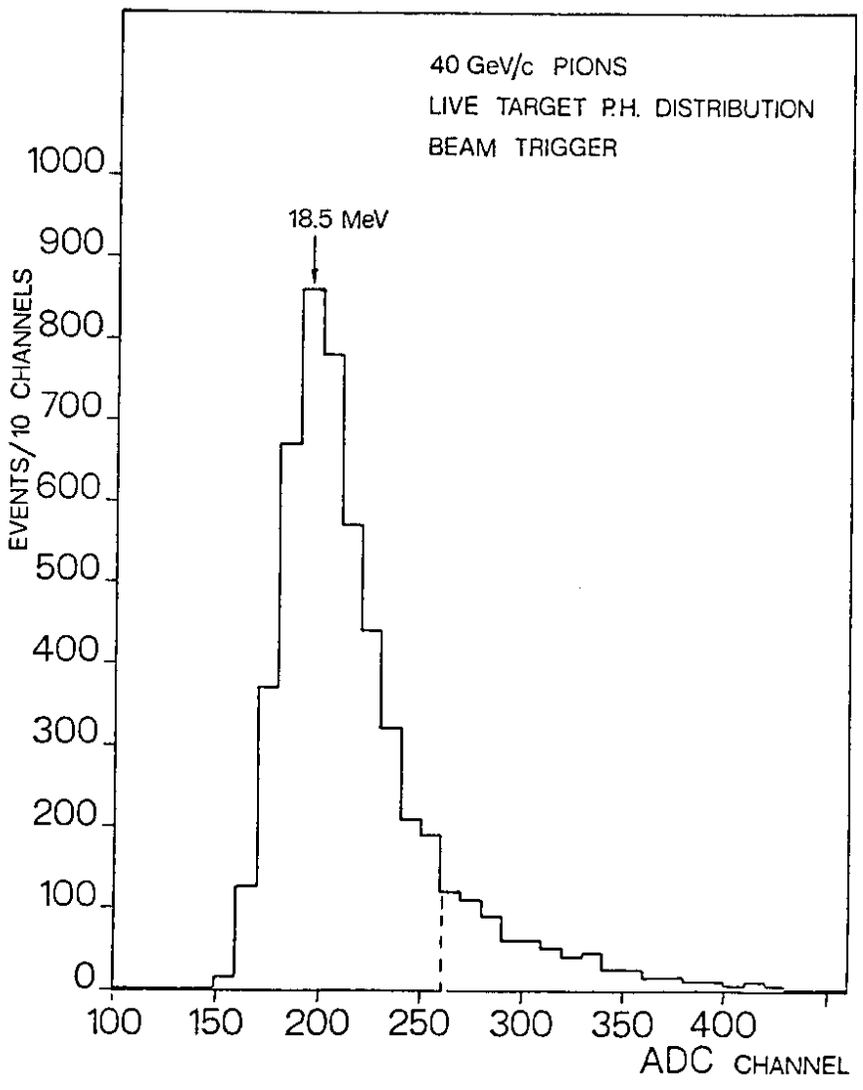
40 GeV/c PIONS
LIVE TARGET P.H. DISTRIBUTION
BEAM TRIGGER
18.5 MeV
EVENTS/10 CHANNELS
1000
900
800
700
600
500
400
300
200
100
0
100
150
200
250
300
350
400
ADC CHANNEL

Fig. 5

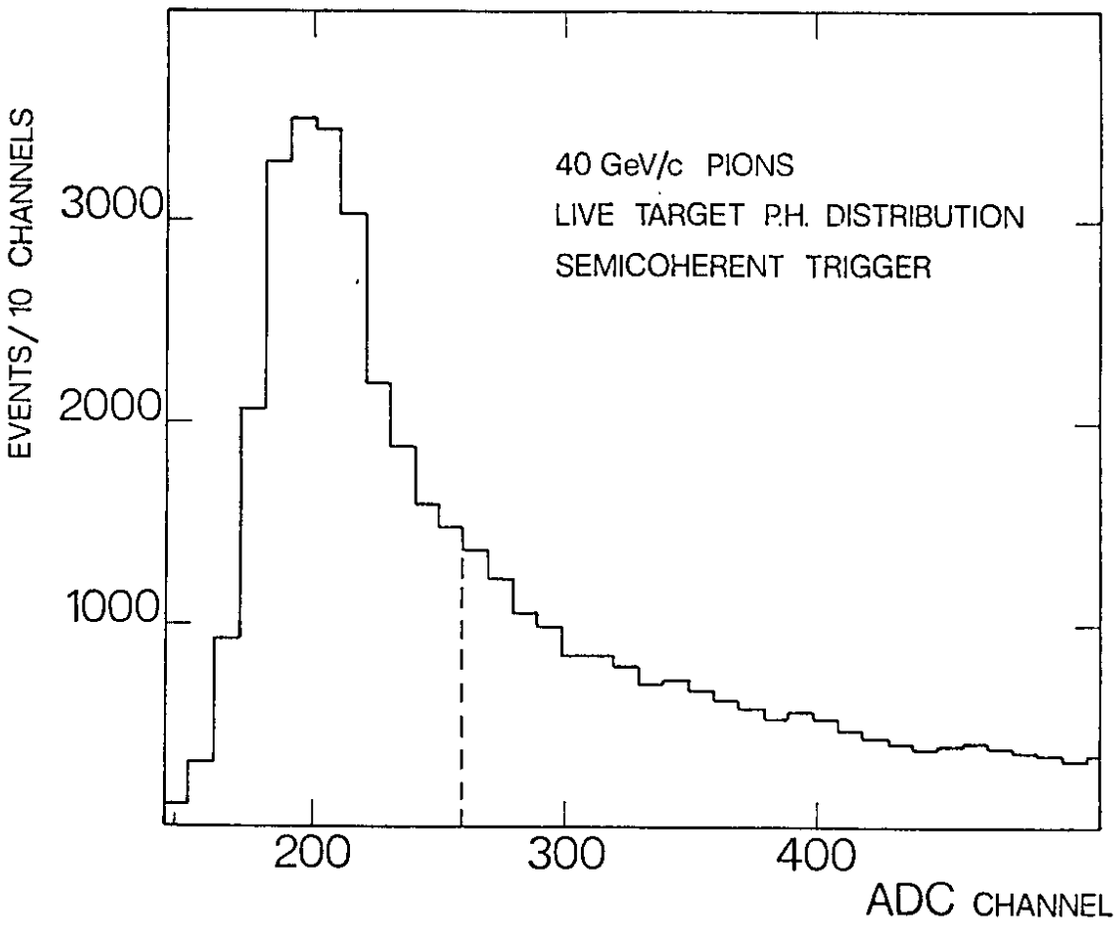
EVENTS/10 CHANNELS
3000
2000
1000
40 GeV/c PIONS
LIVE TARGET P.H. DISTRIBUTION
SEMICOHERENT TRIGGER
200
300
400
ADC CHANNEL

Fig. 6

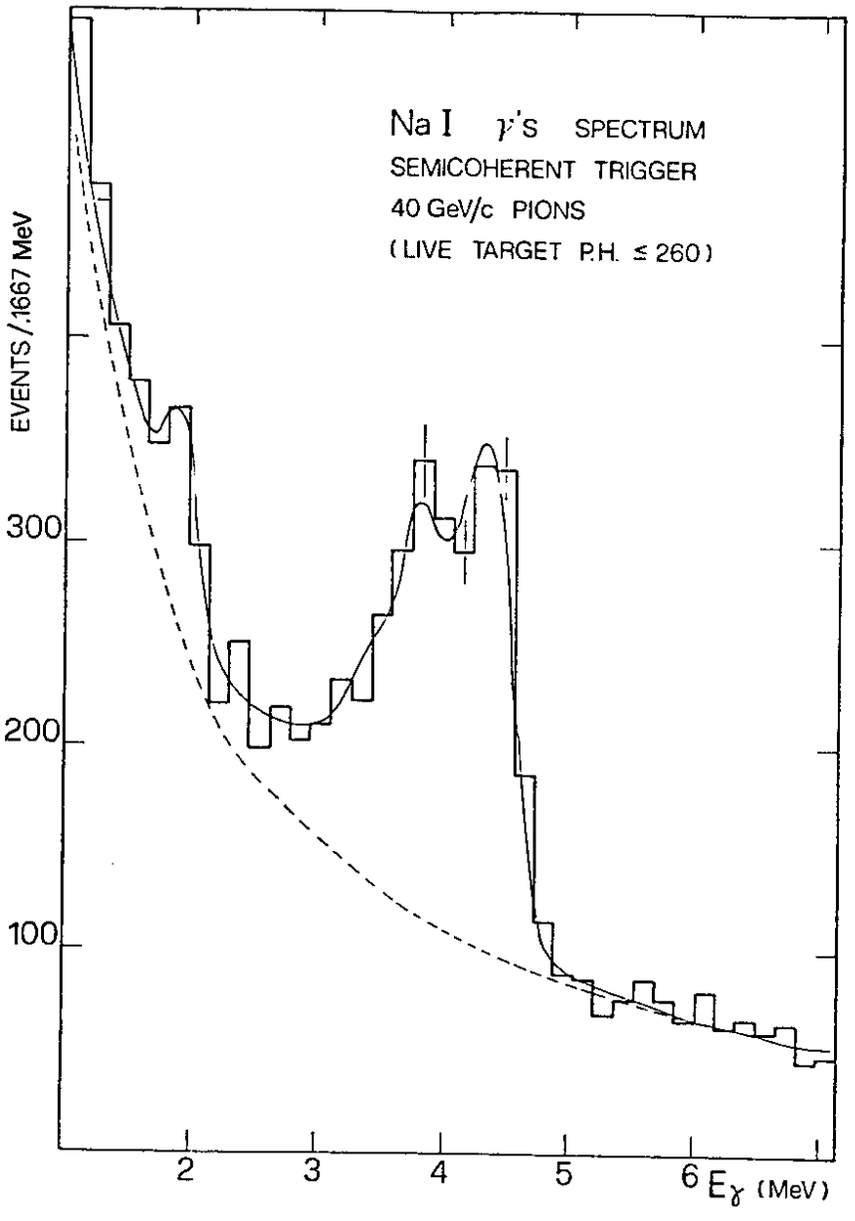
Na I γ's SPECTRUM
SEMICOHERENT TRIGGER
40 GeV/c PIONS
(LIVE TARGET P.H. ≤ 260)
EVENTS/.1667 MeV
300
200
100
2
3
4
5
6
Eγ (MeV)

Fig. 7